IEEE Access
Multidisciplinary | Rapid Review | Open Access Journal

Received August 2, 2018, accepted September 6, 2018, date of publication September 17, 2018, date of current version October 12, 2018.

Digital Object Identifier 10.1109/ACCESS.2018.2870142

A Dual-Band Patch Antenna for Pattern Diversity Application

XINGYU LIU[1], YONGLE WU[2], (Senior Member, IEEE), ZHENG ZHUANG[1], WEIMIN WANG[1], AND YUANAN LIU[1]

[1]Beijing Key Laboratory of Work Safety Intelligent Monitoring, Department of Electronic Engineering, Beijing University of Posts and Telecommunications, Beijing 100876, China
[2]State Key Laboratory of Information Photonics and Optical Communications, School of Electronic Engineering, Beijing University of Posts and Telecommunications, Beijing 100876, China

Corresponding author: Yongle Wu (wuyongle138@gmail.com)

This work was supported in part by the National Natural Science Foundations of China under Grant 61671084, in part by the Guangzhou Major Projects of Industrial Technology of China (Research and Development of Large-scale Multi-beam Antenna Array for 5G Massive MIMO Communication), and in part by the Fund of State Key Laboratory of Information Photonics and Optical Communications (Beijing University of Posts and Telecommunications), China, under Grant IPOC2017ZR06.

ABSTRACT This paper presents a two-port dual-band pattern diversity patch antenna. The antenna consists of a rectangular patch, a rectangular ground plane, and an upright feeding network. The folding microstrip line and the new coplanar waveguide (CPW) structure are printed on two sides of the single feeding network with a size of $35 \times 14.5 \times 1$ mm^3. Therefore, two slots of the new CPW are able to generate in phase and out of phase electric fields, respectively, so that the patch is excited by the even and odd mode in lower common band and by the higher-order modes in upper common band. A prototype of the antenna is fabricated and measured. As a result, the lower common operating frequency band is 14% (2.453–2.821 GHz) and the upper common band is 16% (5.876–6.892 GHz). Moreover, the measured maximum peak gains are 4.0 dBi for Port 1 and 8.6 dBi for Port 2 in the lower common frequency band. In the upper common frequency band, 5.6 dBi for Port 1, and 4.5 dBi for Port 2 are obtained. The satisfactory isolation ($|S_{12}| < -20$ dB) between the two feeding ports in the common impedance matching bands is achieved. The correlation coefficients and the diversity gains have been calculated, which proves the good diversity performance of the antenna.

INDEX TERMS Dual-band antenna, pattern diversity, patch antenna, even/odd mode, CPW feeding.

I. INTRODUCTION

Antenna diversity is a particularly effective solution to deal with multipath situations [1]. Simply, the receiver uses multiple antennas to receive signals from different paths at the same time and then select and merge these signals into a total signal to mitigate the effect of signal fading, which is called antenna diversity. This is the common method to improve the quality and reliability of a wireless link. In the past few years, antenna diversity has arisen great attention due to the function of suppressing multipath fading.

Pattern diversity is one of the ways to realize antenna diversity, which means different patterns combination are excited by two or more co-located antennas. Among the reported pattern diversity patch antenna designs, there are three methods to realize pattern diversity [2]. One is to use a hybrid structure, in other words, the patch antenna is responsible for one radiation pattern, and the other radiation pattern is provided by other structures [3]–[8]. The second way is exciting multiple modes of a single patch by using multiple independent feeding networks [9]–[13]. Compared with single feeding network, multiple independent feeding networks occupy more areas, which makes the size of antenna larger. The third way is exciting the even and odd modes of a single patch [2], [14]–[16]. This method only needs one feeding network, which can shrink the size of antenna and broaden the bandwidth. However, all the projects are single-band designs in the third way, dual-band designs have not yet emerged.

Dual-band or multi-band components [17]–[23] and antennas [24]–[29] are very important for shrinking the size as well as satisfying the rapid growth of users' demand. However, for dual-band pattern diversity patch antenna, it is difficult to use a single feeding network and a single patch to satisfy the various radiating conditions at two frequency bands because the single element limits the freedom of antenna design. As a result, the common method is antenna arrays [27]–[29]. Recently, the designs with radiator printed

on single layer substrate have been presented [25], [26]. The reconfigurable frequency-selective reflectors with a minimum number of switches and two separate feeding networks are used in [25] and [26], respectively. Although the size of radiator has been shrunk, the feeding network is still large.

Based on the broadband design in [2], a new dual-band pattern diversity patch antenna is proposed in this paper. This antenna has a simple structure of a rectangular patch, an upright feeding network and a ground plane. Only a single feeding network and a single patch are utilized to realize pattern diversity in two bands, i.e., four modes. According to simulating by ANSYS HFSS, its S-parameters, radiation patterns and antenna gains were optimized. A prototype of the antenna was fabricated and the results of the measurement and simulation were analyzed.

II. DUAL-BAND PATCH ANTENNA DESIGN

A. ANTENNA STRUCTURE

The geometry of the proposed antenna is shown in Fig. 1. It consists of a rectangular patch, a rectangular ground plane and a FR4-epoxy substrate ($\varepsilon_r = 4.4$, $\tan\delta = 0.02$). The patch and the ground plane are placed parallelly and the substrate is inserted vertically between them. The feeding network is printed on the substrate whose dimension is $35 \times 14.5 \times 1$ mm^3. Both sides of the substrate are printed with feeding circuit.

Fig. 1(c) shows the geometrical configuration of the feeding network. A new CPW transmission line with a T-probe is fed by Port 1 on the front side of the substrate. Compared with traditional CPW, the outer conductor of new CPW is trapezoid and an L-shaped conductor is connected to the top of each side of outer conductor. A T-probe is added to the top of the inner conductor for providing dual-band characteristic by coupled feeding. A fold microstrip line with tapered impedance transformer is fed by Port 2 on the back side. The microstrip line crosses the two slots of CPW to form the structure of microstrip-line-slot. All the dimensions are shown in Table 1.

TABLE 1. Dimensions of the proposed antenna.

Parameter	l_1	l_2	l_3	w_1	w_2	h_1	h_2	h_3
Value (mm)	120	47	35	100	45	14.5	9.5	9
Parameter	d_1	d_2	d_3	d_4	d_5	d_6	d_7	d_8
Value (mm)	16.1	8.7	2	10	10.2	10.2	3.5	1.8
Parameter	m_1	m_2	m_3	m_4	p_1	p_2	p_3	p_4
Value (mm)	4	3.5	0.9	1.5	0.4	0.2	0.3	3.4

B. ANTENNA MECHANISM

In this section, the operating mechanism of the presented antenna is illustrated by comparing it with two reference antennas whose feeding network of the front side are (I) traditional CPW, and (II) traditional CPW with a T-probe, which

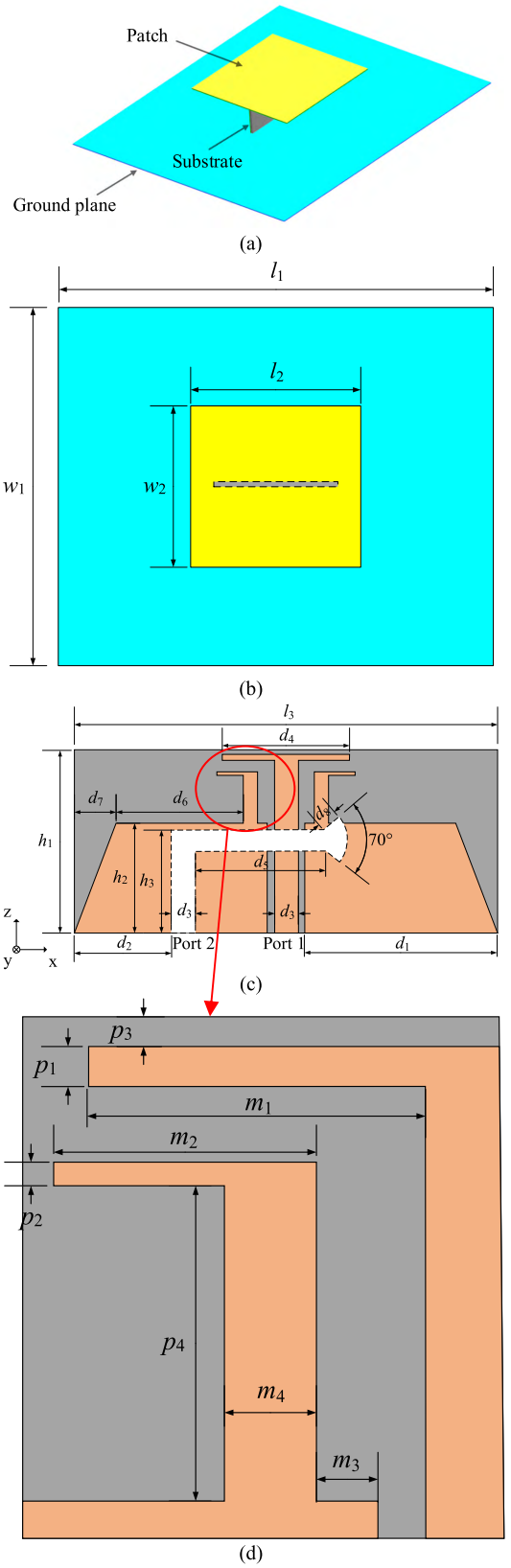

FIGURE 1. The geometry of the proposed antenna. (a)The 3-D exploded view. (b)The top view. (c) The feeding network. (d) The partial enlarged view of the feeding network.

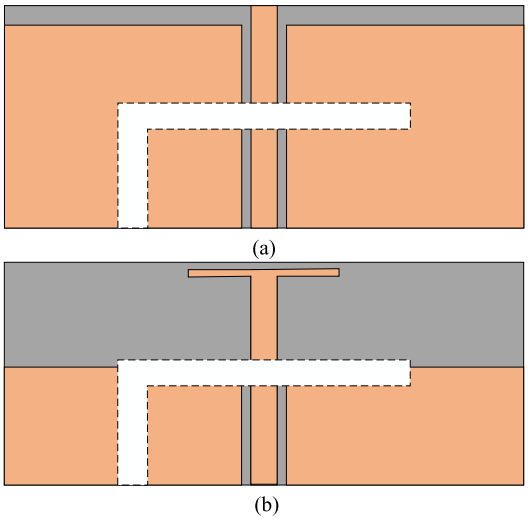

FIGURE 2. The feeding network of reference antennas. (a) Reference Antenna I: traditional CPW. (b) Reference Antenna II: traditional CPW with a T-probe.

can be observed from the Figs. 2(a) and (b). The three antennas have the same dimensions except feeding networks. The corresponding reflection coefficients are shown in Fig. 3. Reference antenna I in [2] has achieved single-band pattern diversity as indicated by the blue line in Fig. 3. Then the aim is to realize dual-band pattern diversity. The idea is to broaden the bandwidth firstly and then to move the expanded bandwidth to higher frequency. The broadband characteristic is achieved by an L-shaped probe in [30]. To make the radiation pattern symmetric, the L-probe is changed into a T-probe. The T-probe needs to keep a distance from the ground, so the height of the CPW decreases because the outer conductor is connected with the ground plane. It is interesting to note that CPW can realize broadband characteristic (78%) by adding a T-shaped probe on the top of the inner conductor. Although broadband has been obtained for $|S_{11}|$, the microstrip-line-slot is unable to feed the patch because the two slots decline with the height of the outer conductor dropped. Therefore, an L-shaped conductor is connected to the top of each side of outer conductor. It is a significant step because the L-shaped conductor sets up the passage of electric fields propagation for the microstrip-line-slot and reduces the distance between the T-probe and the outer conductor partly. Building the passage of electric fields propagation makes the patch fed by Port 2 in two bands. Meanwhile, for the reason of reducing the distance between the T-probe and the outer conductor, the rightward frequency shift is engendered for the expanded bandwidth aroused by T-probe, which separates the expanded bandwidth from lower band and generates upper band characteristic.

A tapered impedance transformer which is connected to the end of microstrip line and the trapezoidal outer conductor are used to achieve impedance matching in two bands. The simulated impedance of the proposed antenna is displayed in Fig. 4.

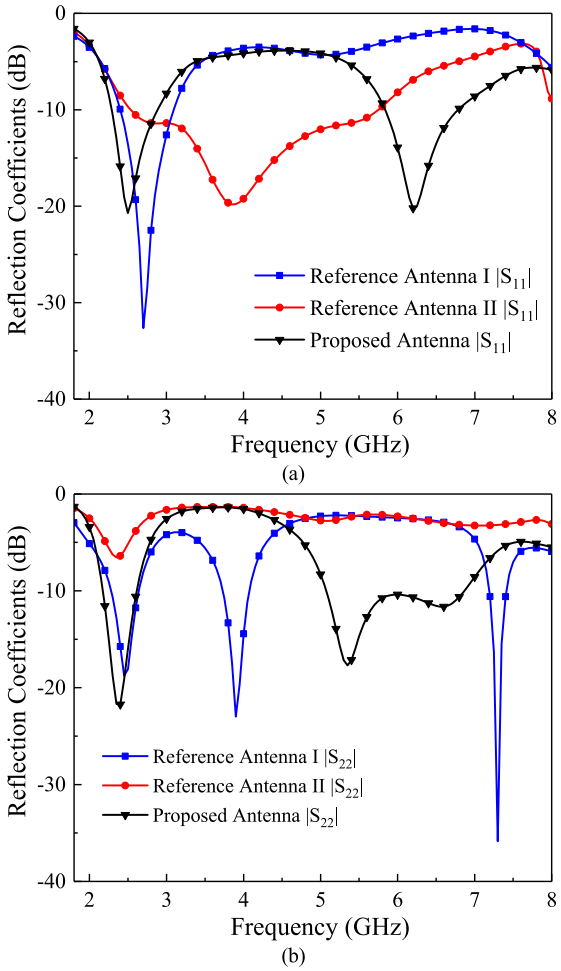

FIGURE 3. Simulated reflection coefficients of the reference and proposed antennas. (a) $|S_{11}|$. (b) $|S_{22}|$.

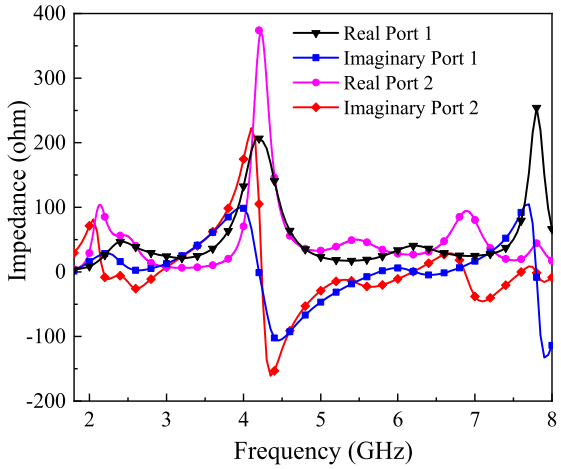

FIGURE 4. Simulated impedance of the proposed antenna.

C. THE ELECTRIC FIELDS DISTRIBUTION

In this section the electric fields distribution of the feeding network is studied. The new CPW includes three parts: one is inner conductor which is equivalent of signal portion,

and others are two outer conductors which work as ground portions. There are two transmission situations: the directions of electric fields are opposite or the same in two slots. Fig. 5 shows the two kinds of electric fields distribution of feeding network. It can be observed that the electric fields in two slots of the CPW are pointed from inner conductor to two outer conductors when Port 1 is excited in Figs. 5(a) and (b), which means that electric fields are out of phase in two slots. In this status the even mode in lower frequency band and the corresponding higher-order mode in upper frequency band of the patch are excited. In Figs. 5(c) and (d), the directions of electric fields in two slots are the same because the microstrip line which crosses the two slots is excited. Therefore, when Port 2 is excited, the electric fields in two slots are the same phase, which indicates that the odd mode in lower frequency band and the corresponding higher-order mode in upper frequency band of the patch are excited.

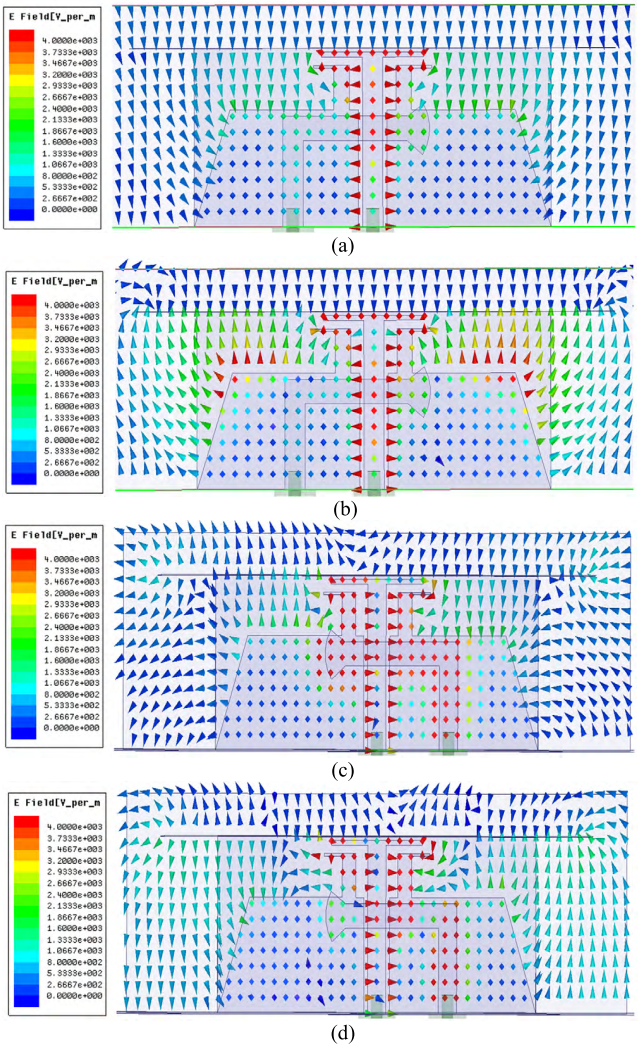

FIGURE 5. The electric fields distribution of the feeding network. (a) Port 1 is excited at 2.5 GHz. (b) Port 1 is excited at 5.98 GHz. (c) Port 2 is excited at 2.5 GHz. (d) Port 2 is excited at 5.98 GHz.

III. SIMULATED AND MEASURED RESULTS

To verify the design, a prototype of the proposed antenna has been fabricated and measured. Fig. 6 shows the photographs of the assembled antenna and the feeding network.

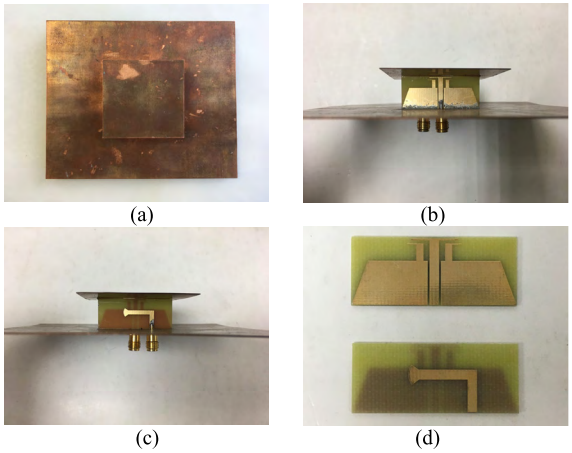

FIGURE 6. The photographs of the proposed antenna. (a) The top view. (b) The side view of the front side. (c)The side view of the back side. (d) The front side and the back side of the feeding network.

It is worth mentioning that the patch and the ground plane are made of copper whose thickness is 0.4 mm. In order to ensure the outer conductor of the new CPW and the ground plane are interconnected, soldering tin is adopted in the joint.

A. S-PARAMETERS

The simulated and measured S-parameters are shown in Figs. 7 and 8. First, the reflection coefficients of lower band are analyzed. It can be seen that the frequency shift appears between the simulated and measured $|S_{11}|$ as well as the excursion is 0.3 GHz approximately. The measured −10 dB bandwidths are 792 MHz (2.453-3.245 GHz) for Port 1 and 802 MHz (2.019-2.821 GHz) for Port 2. The overlapped lower bandwidth is 368 MHz (14%) from

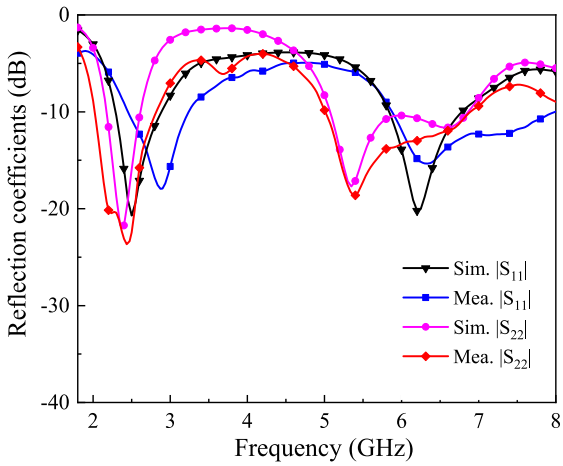

FIGURE 7. The simulated and measured reflection coefficients of the proposed antenna.

2.453 to 2.821 GHz. With regard to upper band, the measured −10 dB operating bands are from 5.876 to 7.995 GHz (2119 MHz) for Port 1 and 5.008 to 6.892 GHz (1748 MHz) for Port 2. The overlapped upper bandwidth is 1016 MHz (16%) from 5.876 to 6.892 GHz. The main cause of fabricated error is the welding between the outer conductor and the ground plane. In simulation the outer conductor of the CPW and the ground plane are connective without welding.

The simulated and measured isolations between Port 1 and Port 2 are depicted in Fig. 8. Due to the electric fields in two slots are 180° out of phase and in phase when two ports excited, the isolation is fairly high. During the two bands the isolation is below −20 dB.

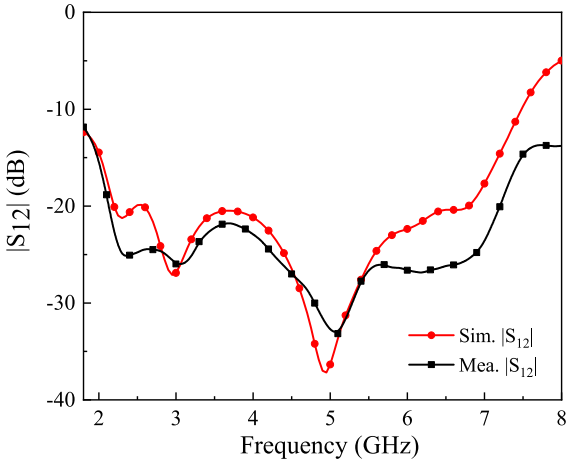

FIGURE 8. The simulated and measured isolations of the proposed antenna.

B. RADIATION PATTERNS

The simulated and measured radiation patterns of the proposed antenna in two bands are shown in Figs. 9 and 10. Because of the limit of measurement conditions, the maximum in upper band only can attain 5.98 GHz. It can be observed that reasonable agreement is obtained between simulated and measured results. When Port 1 is excited, the measured maximum values of co-polarized field are 2.7 dBi at 2.5 GHz and 6.3 dBi at 5.98 GHz. When Port 2 is excited, the measured maximum values of co-polarized field are 8.5 dBi at 2.5 GHz and 4.1 dBi at 5.98 GHz. It is worth noting that the measured realized gains at 2.5 GHz and 5.98 GHz maybe not the maximum values of realized gains in each band and the gains are discussed in section C. The discrepancy of the cross-polarized field is caused by soldering of SMA connectors and the joint between the CPW and the ground plane.

As can be observed from the figures, in lower band the radiation patterns are conical for Port 1 excitation and broadside for Port 2 excitation, which is given rise to the even and the odd modes of the patch. In pattern diversity antennas, the combination of conical and broadside patterns is popular. Furthermore, in the upper band the direction of main-beam

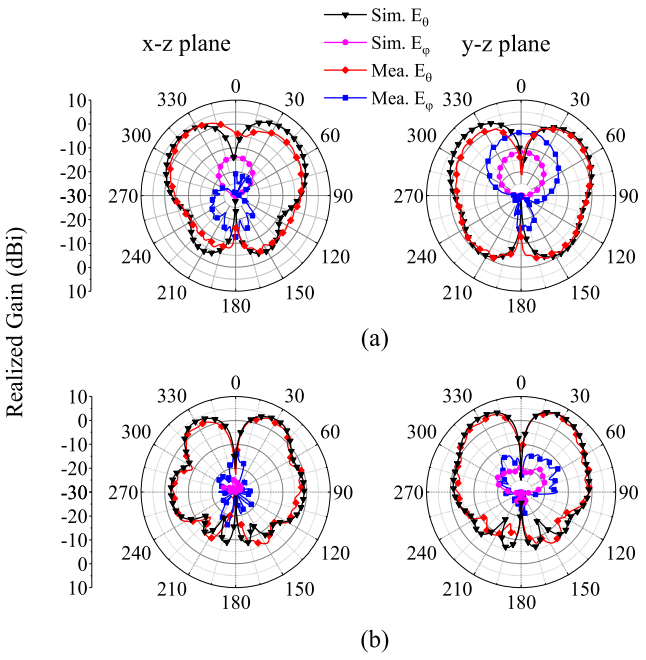

FIGURE 9. The simulated and measured radiation patterns for Port 1 excitation. (a) $f = 2.50$GHz. (b) $f = 5.98$GHz.

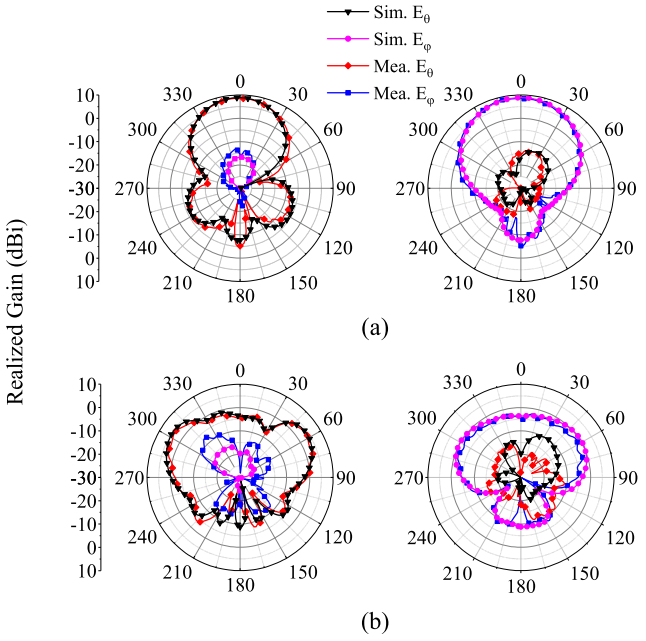

FIGURE 10. The simulated and measured radiation patterns for Port 2 excitation. (a) $f = 2.50$GHz. (b) $f = 5.98$GHz.

is changed with the peak value at the elevation angles of $\theta = 26°$ for Port 1 excitation. As for Port 2, the peak value is at the elevation angles of $\theta = 56°$. The angle difference of the peak value is 30° approximately and the main-beam direction is distinguishing between each other, which meets the need of pattern diversity.

C. GAINS

Figs. 11 and 12 depict the simulated and measured realized gains verse frequency of the proposed antenna. For lower

band, the gain at the point of $\theta = 40°$, $\varphi = 90°$ and the gain in the broadside direction are adopted for Port 1 and Port 2 excitations, respectively. In the operating frequency range, the measured gain varies in the range of 2.0 to 4.0 dBi within the operating band from 2.45 to 2.8 GHz for Port 1. On the other hand, the measured gain for Port 2 excitation is in agreement with the simulated one, except that the measured descending slope is a little high in the operating band, thus resulting in the realized gain varied from 5.0 to 8.6 dBi.

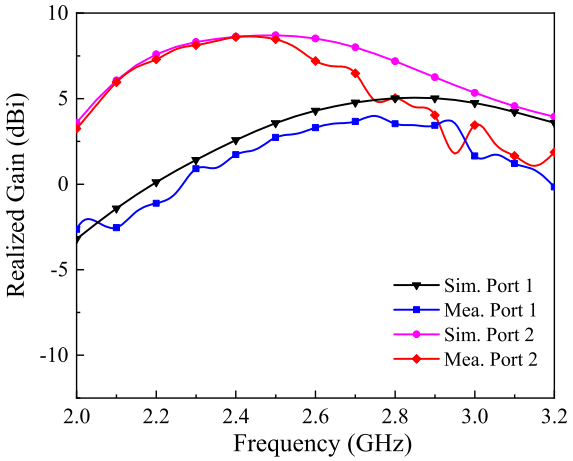

FIGURE 11. The simulated and measured realized gains for lower band.

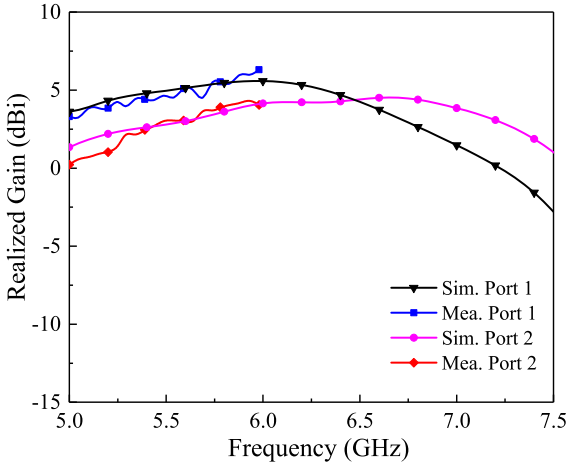

FIGURE 12. The simulated and measured realized gains for upper band.

Fig. 12 displays the realized gains for upper band. The angles appeared in the curves are $\theta = 26°$, $\varphi = 90°$ for Port 1 and $\theta = 56°$, $\varphi = 0°$ for Port 2. The measured realized gains coincide with simulation over a frequency band of 5 to 5.98 GHz. The reason that the realized gains are measured only within this partial band rather than the entire bandwidth is that our measuring equipment provides the operation to the maximum value of 5.98 GHz at present. Over the operating bandwidth scope, the simulated realized gains for Port 1 and Port 2 vary in the range of 2.6 to 5.6 dBi and 3.6 to 4.5 dBi, respectively. For the reason that only partial realized gains are measured in upper band, the other section in this paper adopt the simulated realized gains to reflect the situation of upper band. The performance of the two ports are listed in Table 2.

TABLE 2. Performance of the two ports.

Performance			Bandwidth (GHz)	Maximum realized gain (dBi)
Port1	Lower band	Sim.	2.290-2.885	5.0
		Mea.	2.453-3.245	4.0
	Upper band	Sim.	5.838-6.783	5.6
		Mea.	5.876-7.995	-
Port2	Lower band	Sim.	2.173-2.614	8.7
		Mea.	2.019-2.821	8.6
	Upper band	Sim.	5.073-6.866	4.5
		Mea.	5.008-6.892	-

D. DIVERSITY PERFORMANCE

The diversity performance of the proposed antenna can be evaluated by the correlation coefficient ρ_{12} and diversity gain (DG). According to S-parameters, the ρ_{12} can be calculated [26]

$$\rho_{12} = \frac{|S_{11}^* S_{12} + S_{21}^* S_{22}|}{\sqrt{(1 - |S_{11}|^2 - |S_{21}|^2)(1 - |S_{22}|^2 - |S_{21}|^2)}} \quad (1)$$

The calculated results are shown in Fig. 13. In lower common band, ρ_{12} fluctuates between 0.022-0.048 (0.020-0.025) in simulation (in measurement). As for upper band, the range of variation is 0.007-0.061 (0.007-0.013) in simulation (in measurement). The low correlation coefficients guarantee the excellent performance for diversity application.

The DG can be obtained based on correlation coefficient ρ_{12} [26]

$$\mathrm{DG} = 10\sqrt{1 - \rho_{12}^2} \quad (2)$$

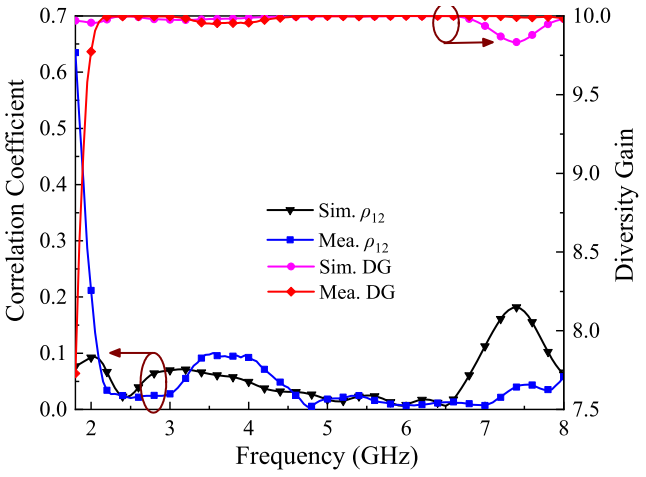

FIGURE 13. The simulated and measured correlation coefficients and diversity gains of the proposed antenna.

TABLE 3. Comparisons of the proposed antenna with other referenced prototypes.

Refs.	Size		Maximum realized gain (dBi)		Bandwidth (%)		Isolation (dB)
	Antenna height (λ)	Feeding network (λ^2)	Lower band	Upper band	Lower band	Upper band	
[25]	0.33	0.46×0.46	3.54/2.08	7.77/4.67	-/19	4.9/3.4	-
[26]	0.06	0.90× 0.90	9.8/5.8	7/1/4.5	7.5	4.5	< -22.3
[27]	0.04	0.41 × 0.41	2.7	2.85	1.7	0.75	< -18.4
[28]	0.0047	0.58 × 0.96	3.59/1.69	7.36/4.52	3.39/6.18	10.2/9.75	< -20
[29]	0.01	0.51 × 0.51	3.80	3.39	12.38	14.57	< -15
Proposed	**0.12**	**0.29 × 0.12**	**4.0/ 8.6**	**5.6/ 4.5**	**14**	**16**	**< -20**

Because only partial realized gains in upper band have been measured, the maximum realized gains in upper band adopt simulation value in Table III.
The two values in one table cell indicate the values of two ports or two modes in one band.
The common bandwidths have been listed in [26] instead of the bandwidths of each port.
λ is the free-space wavelength at the lowest resonant frequency.

The calculated results show that the simulated (measured) diversity gain is above 9.99 (9.99) and 9.98 (9.99) in lower and upper common band, respectively, which confirms the good performance of diversity.

Table 3 lists the comparisons of the proposed antenna with other referenced prototypes. For the reason of adopting the structure of microstrip-line-slot, it is obvious that the size of single-type feeding network is smaller than that of antenna arrays, reconfigurable frequency-selective reflectors or multiple feeding networks. Compared to others designs, the bandwidths, the maximum realized gain and the isolation are pretty good. It is noted that the size of feeding network does not contain the ground plane and the patch, which is adopted in [2].

IV. CONCLUSION

A two-port dual-band patch antenna for pattern diversity application is realized using the odd and even modes and higher-order modes of the patch. The four modes are excited by a single compact feeding network with a size of $35 \times 14.5 \times 1$ mm^3, a single patch and a ground plane. The principle of dual-band characteristic has been researched above. The maximized overlapped −10 dB impedance bandwidths achieve 14% for lower common band, 16% for upper common band and the isolation is less than −20 dB in both bands. From the simulated and measured results, it is found that the main-beam positions of the radiation patterns are directed at the elevation angles of 40°, 0° for lower band and 26°, 56° for upper band respectively. As for the diversity performance, the simulated and measured correlation coefficients are fairly low and the diversity gains are higher than 9.98 in both bands, which satisfies pattern diversity application.

REFERENCES

[1] M. R. Kamarudin, Y. I. Nechayev, and P. S. Hall, "Onbody diversity and angle-of-arrival measurement using a pattern switching antenna," *IEEE Trans. Antennas Propag.*, vol. 57, no. 4, pp. 964–971, Apr. 2009.
[2] C. Deng, Y. Li, X. Lv, and Z. Feng, "Wideband dual-mode patch antenna with compact CPW feeding network for pattern diversity application," *IEEE Trans. Antennas Propag.*, vol. 66, no. 5, pp. 2628–2633, May 2018.
[3] X. Gao, H. Zhong, Z. Zhang, Z. Feng, and M. F. Iskander, "Low-profile planar tripolarization antenna for WLAN communications," *IEEE Antennas Wireless Propag. Lett.*, vol. 9, pp. 83–86, 2010.
[4] R. Masood, C. Person, and R. Sauleau, "A dual-mode, dual-port pattern diversity antenna for 2.45-GHz WBAN," *IEEE Antennas Wireless Propag. Lett.*, vol. 16, pp. 1064–1067, 2017.
[5] L. Sun, W. Huang, B. Sun, Q. Sun, and J. Fan, "Two-port pattern diversity antenna for 3G and 4G MIMO indoor applications," *IEEE Antennas Wireless Propag. Lett.*, vol. 13, pp. 1573–1576, 2014.
[6] H. Zhong, Z. Zhang, W. Chen, Z. Feng, and M. F. Iskander, "A tripolarization antenna fed by proximity coupling and probe," *IEEE Antennas Wireless Propag. Lett.*, vol. 8, pp. 465–467, 2009.
[7] J. Oh and K. Sarabandi, "Compact, low profile, common aperture polarization, and pattern diversity antennas," *IEEE Trans. Antennas Propag.*, vol. 62, no. 2, pp. 569–576, Feb. 2014.
[8] N. Herscovici, C. Christodoulou, E. Rajo-Iglesias, O. Quevedo-Teruel, and M. Sanchez-Fernandez, "Compact multimode patch antennas for MIMO applications [wireless corner]," *IEEE Antennas Propag. Mag.*, vol. 50, no. 2, pp. 197–205, Apr. 2008.
[9] K. Wei, Z. Zhang, W. Chen, and Z. Feng, "A compact CPW-FED circular patch antenna with pattern and polarization diversities," *Microw. Opt. Technol. Lett.*, vol. 53, no. 5, pp. 968–972, May 2011.
[10] S. L. S. Yang and K. M. Luk, "Design of a wide-band L-probe patch antenna for pattern reconfiguration or diversity applications," *IEEE Trans. Antennas Propag.*, vol. 54, no. 2, pp. 433–438, Feb. 2006.
[11] K. Wei, Z. Zhang, W. Chen, and Z. Feng, "A novel hybrid-fed patch antenna with pattern diversity," *IEEE Antennas Wireless Propag. Lett.*, vol. 9, pp. 562–565, 2010.
[12] S. L. S. Yang, K. M. Luk, H. W. Lai, A. A. Kishk, and K. F. Lee, "A dual-polarized antenna with pattern diversity," *IEEE Antennas Propag. Mag.*, vol. 50, no. 6, pp. 71–79, Dec. 2008.
[13] L. Cui, W. Wu, and D. G. Fang, "Wideband circular patch antenna for pattern diversity application," *IEEE Antennas Wireless Propag. Lett.*, vol. 14, pp. 1298–1301, 2015.
[14] K. Krishnamoorthy, B. Majumder, J. Mukherjee, and K. P. Ray, "Low profile pattern diversity antenna using quarter-mode substrate integrated waveguide," *Prog. Electromagn. Res. Lett.*, vol. 55, pp. 105–111, 2015.
[15] L. Sun, G.-X. Zhang, B.-H. Sun, W.-D. Tang, and J.-P. Yuan, "A single patch antenna with broadside and conical radiation patterns for 3G/4G pattern diversity," *IEEE Antennas Wireless Propag. Lett.*, vol. 15, pp. 433–436, 2015.
[16] X. Jiang, Z. Zhang, Y. Li, and Z. Feng, "A novel null scanning antenna using even and odd modes of a shorted patch," *IEEE Trans. Antennas Propag.*, vol. 62, no. 4, pp. 1903–1909, Apr. 2014.
[17] Y. Wu, L. Cui, Z. Zhuang, W. Wang, and Y. Liu, "A simple planar dual-band bandpass filter with multiple transmission poles and zeros," *IEEE Trans. Circuits Syst. II, Exp. Briefs*, vol. 65, no. 1, pp. 56–60, Jan. 2018.
[18] P. Ma, B. Wei, J. Hong, X. Guo, B. Cao, and L. Jiang, "Coupling matrix compression technique for high-isolation dual-mode dual-band filters," *IEEE Trans. Microw. Theory Techn.*, vol. 66, no. 6, pp. 2814–2821, Jun. 2018.
[19] B. Ren *et al.*, "Compact dual-band differential bandpass filter using quadruple-mode stepped-impedance square ring loaded resonators," *IEEE Access*, vol. 6, pp. 21850–211858, 2018.
[20] N. Sekiya and T. Unno, "Independently tunable HTS dual-band bandpass filters using dielectric rods," *IEEE Trans. Appl. Supercond.*, vol. 28, no. 4, Jun. 2018, Art. no. 1500105.

[21] R. Gómez-García, J. Rosario-De Jesus, and D. Psychogiou, "Multi-band bandpass and bandstop RF filtering couplers with dynamically-controlled bands," *IEEE Access*, vol. 6, pp. 32321–32327, 2018.
[22] R. Gómez-García, R. Loeches-Sánchez, D. Psychogiou, and D. Peroulis, "Single/multi-band Wilkinson-type power dividers with embedded transversal filtering sections and application to channelized filters," *IEEE Trans. Circuits Syst. I, Reg. Papers*, vol. 62, no. 6, pp. 1518–1527, Jun. 2015.
[23] K. Zhou, C. Zhou, and W. Wen, "Substrate-integrated waveguide dual-band filters with closely spaced passbands and flexibly allocated bandwidths," *IEEE Trans. Compon., Packag., Manuf. Technol.*, vol. 8, no. 3, pp. 465–472, Mar. 2018.
[24] K. Dhwaj, H. Tian, and T. Itoh, "Low-profile dual-band filtering antenna using common planar cavity," *IEEE Antennas Wireless Propag. Lett.*, vol. 17, no. 6, pp. 1081–1084, Jun. 2018.
[25] C.-H. Ko, I.-Y. Tarn, and S.-J. Chung, "A compact dual-band pattern diversity antenna by dual-band reconfigurable frequency-selective reflectors with a minimum number of switches," *IEEE Trans. Antennas Propag.*, vol. 61, no. 2, pp. 646–654, Feb. 2013.
[26] S. Yan and G. A. E. Vandenbosch, "Low-profile dual-band pattern diversity patch antenna based on composite right/left-handed transmission line," *IEEE Trans. Antennas Propag.*, vol. 65, no. 6, pp. 2808–2815, Jun. 2017.
[27] A. Boukarkar, X. Q. Lin, Y. Jiang, L. Y. Nie, P. Mei, and Y. Yu, "A miniaturized extremely close-spaced four-element dual-band MIMO antenna system with polarization and pattern diversity," *IEEE Antennas Wireless Propag. Lett.*, vol. 17, no. 1, pp. 134–137, Jan. 2018.
[28] D. Sarkar, K. Saurav, and K. V. Srivastava, "Dual band complementary split-ring resonator-loaded printed dipole antenna arrays for pattern diversity multiple-input–multiple-output applications," *IET Microw. Antennas Propag.*, vol. 10, no. 10, pp. 1113–1123, Jul. 2016.
[29] D. Sarkar, K. Saurav, and K. V. Srivastava, "A compact four element CSRR-loaded antenna for dual band pattern diversity MIMO applications," in *Proc. 46th Eur. Microw. Conf. (EuMC)*, London, U.K., Oct. 2016, pp. 1315–1318.
[30] Y.-X. Guo, K.-M. Luk, and K.-F. Lee, "Broadband dual polarization patch element for PCS base stations," in *Proc. Asia–Pacific Microw. Conf.*, Dec. 2000, pp. 1369–1372.

XINGYU LIU received the B.S. degree in electronic science and technology from the Taiyuan University of Science and Technology, Taiyuan, China, in 2017. He is currently pursuing the M.S. degree with the Beijing University of Posts and Telecommunications, Beijing, China. His research interests include pattern diversity antennas and filtering antennas.

YONGLE WU (M'12–SM'15) received the B.Eng. degree in communication engineering and the Ph.D. degree in electronic engineering from the Beijing University of Posts and Telecommunications (BUPT), Beijing, China, in 2006 and 2011, respectively.

In 2010, he was a Research Assistant with the City University of Hong Kong (CityU), Hong Kong. He joined BUPT in 2011, where he is currently a Full Professor with the School of Electronic Engineering. His research interests include microwave components, circuits, antennas, and wireless systems design.

ZHENG ZHUANG received the B.S. degree in electronic science and technology from the Beijing University of Chemical Technology, Beijing, China, in 2015. In 2015, he started his research as a graduate with the Beijing University of Posts and Telecommunications, where he is currently pursuing the the Ph.D. degree.

His research interests include microwave passive components, power amplifiers, and transformation optics.

WEIMIN WANG received the B.S. degree in communication engineering, the M.S. degree in electromagnetic field and microwave technology, and the Ph.D. degree in electronic science and technology from Beijing University of Posts and Telecommunications (BUPT), Beijing, China, in 1999, 2004, and 2014, respectively. She joined BUPT in 2014, where she is currently a Lecturer with the School of Electronic Engineering. Her research interests include electromagnetic field and MIMO OTA measurement.

YUANAN LIU received the B.E., M.Eng., and Ph.D. degrees in electrical engineering from the University of Electronic Science and Technology of China, Chengdu, China, in 1984, 1989, and 1992, respectively.

In 1984, he joined the 26th Institute of Electronic Ministry of China to develop the inertia navigating system. In 1992, he began his first post-doctoral position at the EMC Laboratory, Beijing University of Posts and Telecommunications (BUPT), Beijing, China. In 1995, he started his second post-doctoral at the Broadband Mobile Laboratory, Department of System and Computer Engineering, Carleton University, Ottawa, Canada. Since 1997, he has been a Professor with the Wireless Communication Center, College of Telecommunication Engineering, BUPT, where he is involved in the development of next-generation cellular systems, wireless LANs, Bluetooth applications for data transmission, EMC design strategies for high-speed digital systems, and EMI and EMS measuring sites with low-cost and high-performance.